Journal of Medicinal Chemistry

Article

The Discovery of Azaindole Ureas as a Novel Class of Bacterial Gyrase B Inhibitors

Jing Zhang, Qingyi Yang, Jason B Cross, Jan A Romero, Katherine M Poutsiaka, Felix Epie, Douglas Bevan, Bin Wang, Yanzhi Zhang, Xin Zhang, Anu Daniel, Moy Terence, Kien Nguyen, Brian P Chamberlain, Nicole Carter, Ajit Chavan, Joseph Shotwell, Jared a Silverman, Chester A Metcalf, Dominic M Ryan, Blaise Lippa, and Roland E Dolle

J. Med. Chem., **Just Accepted Manuscript** • DOI: 10.1021/acs.jmedchem.5b00961 • Publication Date (Web): 13 Oct 2015

ACS Publications

Journal of Medicinal Chemistry is published by the American Chemical Society. 1155 Sixteenth Street N.W., Washington, DC 20036

The Discovery of Azaindole Ureas as a Novel Class of Bacterial Gyrase B Inhibitors

Jing Zhang[*], *Qingyi Yang, Jason Cross, Jan Antoinette C. Romero, Katherine M. Poutsiaka, Felix Epie, Douglas Bevan, Bin Wang, Yanzhi Zhang, Ajit Chavan, Xin Zhang, Terence Moy, Anu Daniel, Kien Nguyen, Brian Chamberlain, Nicole Carter, Joseph Shotwell, Jared Silverman, Chester A. Metcalf, III, Dominic Ryan, Blaise Lippa, Roland E. Dolle*

Cubist Pharmaceuticals Inc., Lexington, Massachusetts 02421, USA

ABSTRACT: The emergence and spread of multidrug-resistant bacteria are widely believed to endanger human health. New drug targets and lead compounds exempt from cross-resistance with existing drugs are urgently needed. We report on the discovery of azaindole ureas as a novel class of bacterial gyrase B inhibitors and detail the story of their evolution from a *de novo* design hit based on structure based drug design. These inhibitors show potent MICs against fluoroquinolone resistant *MRSA* and other Gram-positive bacteria.

INTRODUCTION

Due to the increasing prevalence of bacterial antibiotic resistance, the current available antibiotics continue to lose their efficacy. Therefore, the investigation and development of new antibacterials that avoid the existing mechanisms of resistance offer a solution to this growing unmet medical need. Bacterial DNA type II topoisomerases are well-established targets for both

Gram-positive and Gram-negative bacteria. The GyrA subunit of the DNA Gyrase complex is the target for fluoroquinolones. The GyrB subunit, the target of Novobiocin, offers an opportunity for overcoming the widespread cross-resistance to fluoroquinolones. Due to the clinical success of the fluoroquinolone class of antibacterials, GyrB has attracted a great deal of interest from both industrial and academic institutions[1-4]. Some representative GyrB inhibitors are depicted in Figure 1: the tricyclic pyrimidines **1a** from Trius[5], aminobenzimidazoles **1b** from Vertex[6-7], cyclothialidines **1c**[8-9] pyrrolamides **1d** from Astra-Zeneca[10-12] and imidazolopyridine **1e** from Pfizer[13]. Herein we wish to report the evolution of azaindole ureas as a novel class of GyrB inhibitors from our *de novo* design starting point **1f**.

RESULTS AND DISCUSSION

Chemistry. The de novo design starting point aminothiazole **1f** was synthesized from commercially available 1*H*-pyrrole-2-carbaldehyde **2** (**Scheme 1**). After the indole NH protection as its tosylate **3**, condensation with methyl *N,N*-dimethylaminoacetate gave α-ketoester **4** in an unoptimized 15% yield, which upon cyclization with thiourea provided the key intermediate **5** in 28% yield. Urea formation with ethylisocyanate yielded **6** in 67% yield, which was converted into **1f** via $LiAlH_4$ mediated ester reduction and tosylate deprotection in one pot in 8% overall yield.

The synthesis of azaindole derivatives is quite straightforward starting from the commercial 6-bromo-3-nitro-4-azaindole **8** (**Scheme 2**)[14]. Iron powder mediated nitro reduction, followed by treating with ethylisocyanate gave **10** in 75% overall yield. Suzuki coupling provided the NH unsubstituted parent azaindole **11** in 66% isolated yield. Alternatively, SN_{Ar} reaction of **10** with

2-fluoropyridine and the subsequent Suzuki coupling provided analog **12** in 43% and 63% yields, respectively. The syntheses of all the azaindole analogs follow this general synthetic route.

Discussion. Compound **1f** was discovered as a promising medicinal chemistry starting point using structure based *de novo* virtual design and the subsequent preliminary analoging efforts. It has an IC_{50} of 2.5 uM against *Staphylococcus* GyrB with high ligand efficiency. In addition, it also demonstrates weak antibacterial activity with an MIC of 128 ug/mL and 16 ug/mL vs *MSSA* and *Streptococcus pneumoniae.* We were able to resolve the X-ray structure of compound **1f** bound in the ATPase pocket of a 24kDa portion of the *Staphylococcus* GyrB protein (**Figure 2**, PDB code 5D6P). The co-crystal structure revealed the following binding features: 1) a hydrogen bond donor-acceptor interaction network between the thiazole urea (thiazole ring N, two urea NH), catalytic Asp81 and a conserved water molecule, which is stabilized by the hydrogen bond interactions with Asp81, Gly85 and Thr173; 2) the ethyl fits snugly in the small lipophilic pocket; 3) the hydroxyl has a HB with Glu58 while also forming an intramolecular HB with pyrrole NH, helping to restrict the pyrrole conformation; 4) the pyrrole sits in the open binding pocket surrounded by lipophilic residues such as Ile86 and Pro87; 5) there is no contact with Arg84 and Arg144. It has been well known that engaging these two Args could dramatically improve the enzymatic activity of an inhibitor[1-4]. From the X-ray structure, it is clear that the C4-thiazole substituent projects toward the two arginines, and the C5-substituent is near the lipophilic pocket while also offering opportunities to engage the two arginines.

With compound **1f** as our medicinal chemistry starting point, we undertook extensive SAR studies around the thiazole ring[15]. Surprisingly, the SAR around the C2, C4 and C5 positions were very flat (data not shown). For C2 substitution, the ethylurea is the best group to occupy the

small lipophilic pocket (**Figure 2**). For C5 substitution, small substituents lead to a decrease of binding potency while larger groups such as aryls or biaryls are preferred, however with rather flat SAR. Due to the spatial arrangement of the C5 substitution in the protein pocket, we were never able to engage any meaningful interactions with Arg84 and Arg144 residues. Therefore, any apparent 2-3X increases in binding potency was neutralized by the increase in molecular weight and overall clogP.

Significant medicinal and computational chemistry efforts were then directed toward the C4 position to try to engage the two Arg redidues. Although a rather flat SAR was developed here again, compound **7** caught our attention as its GyrB cocrystal structure showed the pyridine indeed engaged the two Arg residues via a hydrogen bond and a π-cation stacking interaction (**Figure 3**, PDB code 5D6Q). The C5 pyrrole was again positioned in the lipophilic pocket. The thiazole nitrogen together with the two urea NHs formed the characteristic hydrogen bond network with Asp81 via the conserved water molecule. We realized that there was a non-conserved water molecule forming a hydrogen bond to the thiazole nitrogen in the open binding pocket adjacent to the Asp81 hydrogen bond network. It was envisaged that if we could fuse a heterocycle to the thiazole with an appropriately placed heteroatom to displace the non-conserved water molecule, we should be able to improve the binding affinity significantly (**Figure 4**). Based on molecular modeling and synthetic feasibility, we chose azaindole as the core scaffold to test this hypothesis.

Although the parent azaindole analog **11** only showed similar GyrB IC_{50} to thiazole analog **7**, possibly due to the loss of pyrrole lipophilic interactions, it was gratifying to find out that the novel analog **12** showed ~40X IC_{50} improvement over **7** with improved ligand efficiency.

Moreover, **12** showed an MIC of 16 ug/mL vs a *MRSA* strain. We were then able to resolve the X-ray co-crystal structure of **12** complexed with GyrB (**Figure 5**, PDB code 5D7C). The pyridine nitrogen indeed displaces the non-conserved water molecule as designed. In addition, the pyridine nitrogen along with one of the urea NHs form a water mediated hydrogen bond network with Asp81. We realized that the other urea NH sits a bit further from the Asp81 carbonyl and could not form a bifurcated hydrogen bond as in Vertex's urea analog[3]. This non-optimized hydrogen bonding could offer an opportunity for further potency improvement if both NHs could be engaged. As predicted, the C6-pyridine forms a hydrogen bond and π-cation stacking interaction with the two Arg residues. The para position of the pyridine ring projects toward the solvent exposed area, offering an opportunity to incorporate polar functional groups to improve the overall physiochemical properties. The N1-pyridine adopts a small dihedral angle with respect to the parent azaindole core, and sits in the upper lipophilic pocket.

With Azaindole urea **12** identified as a novel GyrB inhibitor, we carried out detailed SAR studies around the azaindole scaffold. The azaindole N1 aryl SAR is detailed in **Table 1**. Realizing that the 2-pyridyl adopts a small dihedral angle in regards to the azaindole bicycle, we anticipate that the 2-pyrimidyl substitution would partially relieve the torsional strain between the aryl and azaindole, potentially improving the potency due to substrate preorganization. Analog **13** is indeed ~2X more potent in both IC_{50} and MIC than **12**. Analog **14**, with increased torsional strain, is 10X less potent than **12**, further substantiating the torsional strain hypothesis. Further SAR studies were thus based on 2-pyrimidyl substitution. While 4-substituted pyrimidine analogs **15**-**19** show potent GyrB inhibition, they all show poor MICs except **19**. 5-Pyrimidine substitution shows intriguing SARs with regard to electronic properties of the substituents. Small electron-donating substituents are all tolerated. 5-Methylpyrimidine analog **20** improves the IC_{50}

and MIC by 2X over **13**. The corresponding ethyl and methoxy analogs **21** and **22** have similar profiles to **13**. 5-Halopyrimidines **23**-**25** all display a similar GyrB IC_{50}. Though 5-fluoropyrimidine **23** gives disappointing MICs, the corresponding chloro- and bromo-derivatives **24** and **25** display a very impressive level of MICs across the Gram+ MIC panel including a fluoroquinolone resistant *MRSA* strain. The improved MIC profile of these halo-analogs is probably due to enhanced bacterial cell penetration. 5-Substituents with electron-withdrawing properties such as **26** and **27** in general show poor MICs. Though **26** with a small 5-CN shows 18 nM GyrB potency, slightly larger 5-CF_3 analog **27** is totally inactive, consistent with a small tight binding pocket around the 5-pyrimidine position as shown in the X-ray cocrystal structure.

In order to further improve the physiochemical properties of the azaindole analogs, we also explored the nonaryl substitutions as shown in **Table 2**. In the **12**-GyrB cocrystal structure (**Figure 5**), the coplanar arrangement of the 2-pyridine and azaindole bicycle is the preferred binding conformation. It is therefore not surprising that steep SAR was observed (**Table 1**). Most of the analogs show GyrB binding potency in the micromolar range with a few exceptions such as those carrying unsaturation in **31**, **33** and **38**. N-cyclohexyl analog **34** is also worth noting due to the marginal potency loss from 2-pyridyl analog **12**. Interestingly, moderately active acrylate analog **38** could serve as a tool compound to explore covalent GyrB inhibitors due to the reactive acrylate warhead.

With N1 substituents optimized, we next turned our attention to the C6 aryl region (**Table 3**). The goal was to optimize the interactions of the aryl with the two Arg residues and improve the overall physiochemical properties for better ADME profile. Cyanopyrimidine analog **39** gave

potent GyrB inhibition with rather poor MICs. 2-Fluoropyridyl derivative **40** lost enzymatic activity dramatically, possibly due to the perturbation of the dihedral angle induced by the fluorine. Compound **41** adopted from Vertex's Gyrase program showed great enzymatic activity and 2X MIC improvements over **12**. N-methylpyridone derivative **42** gave substantially improved IC_{50} and 4X MIC improvements over **12**, clearly demonstrating the superiority of the pyridone moiety over pyridine to interact with the two Arginine residues and improve the overall cell penetration properties. Our strategy to combine N-methylpyridone with the best azaindole N-substitutions resulted in the discovery of **44**-**46** with excellent MIC profile across the Gram+ MIC panel including a fluoroquinolone resistant *MRSA* strain, a *Streptococcus pneumoniae* strain, and two *Enterococcus* strains. Surprisingly, N-hydroxyethylpyridone analog **47** gave much poorer MIC profile relative to N-methyl analog **46**.

CONCLUSION

In summary, using structure based drug design, we were able to quickly analyze the SAR around our *de novo* starting compound **1f** and design a series of more potent and novel azaindole-based gyrase B inhibitors. Our strategy evolved to displace a non-conserved water molecule identified in the co-crystal structure of **7**. Further SAR studies around the azaindole core resulted in the discovery of a number of potent gyrase B inhibitors with excellent Gram+ MIC profiles. There is virtually no MIC shift between quinolone susceptible and resistant *MRSA* strains for all our GyrB inhibitors. These molecules could provide great utility in the fight against fluoroquinolone resistance. Further *in vitro* and *in vivo* characterization of a few select azaindoles will be reported in a future publication.

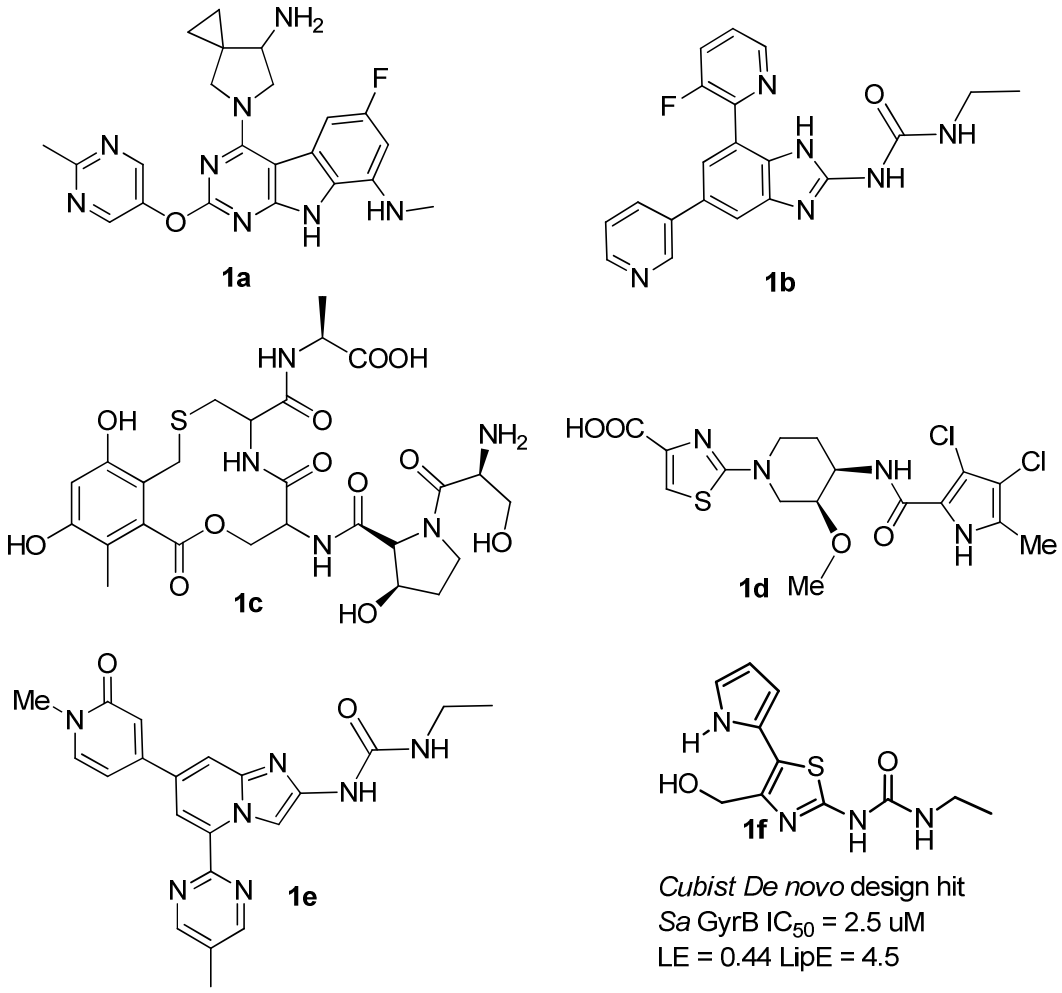

Figure 1. Structures of some representative GyrB inhibitors

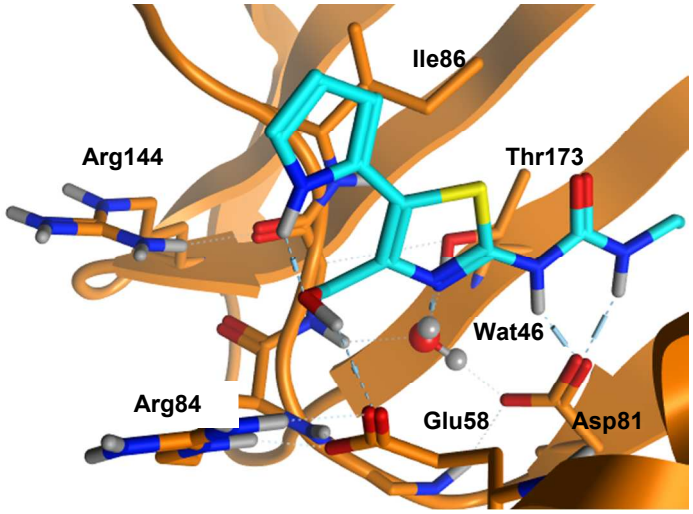

Figure 2. X-ray crystal structure of **1f** bound to the 24 kDa *Sa* GyrB ATPase active site (1.6 Å, PDB code 5D6P)

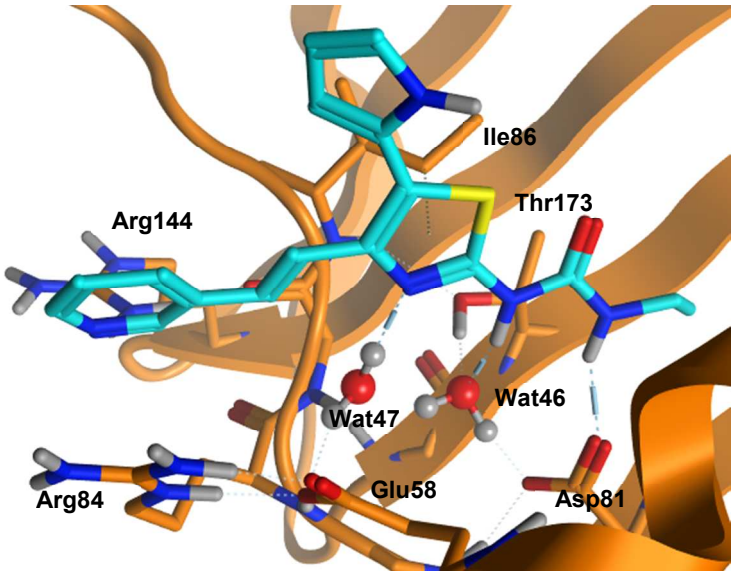

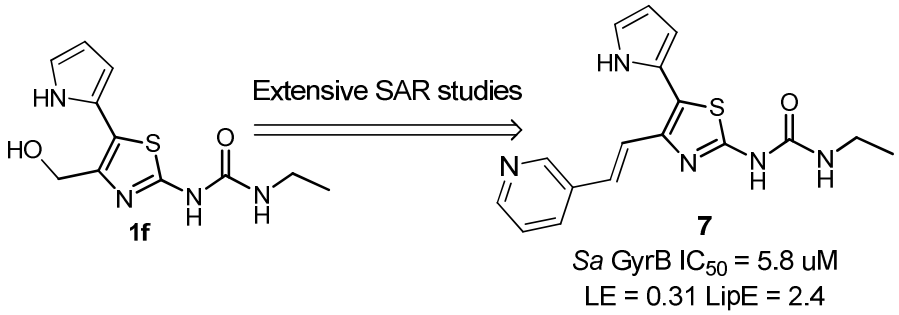

Figure 3. Structure of **7** and its X-ray structure with 24 kDa *Sa* GyrB ATPase (PDB code 5D6Q)

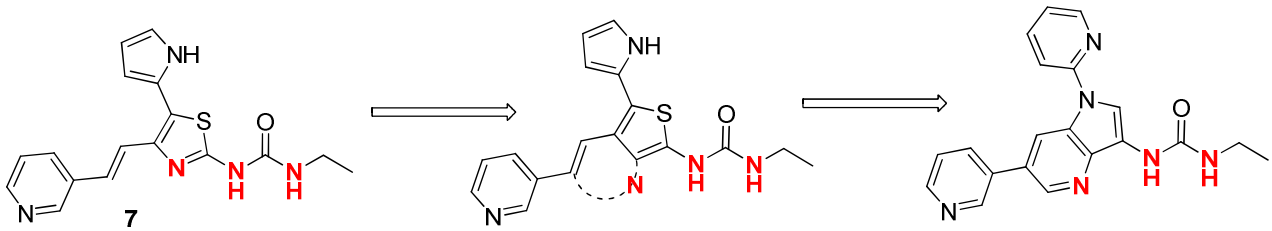

Figure 4. Working hypothesis leading to the azaindole scaffold

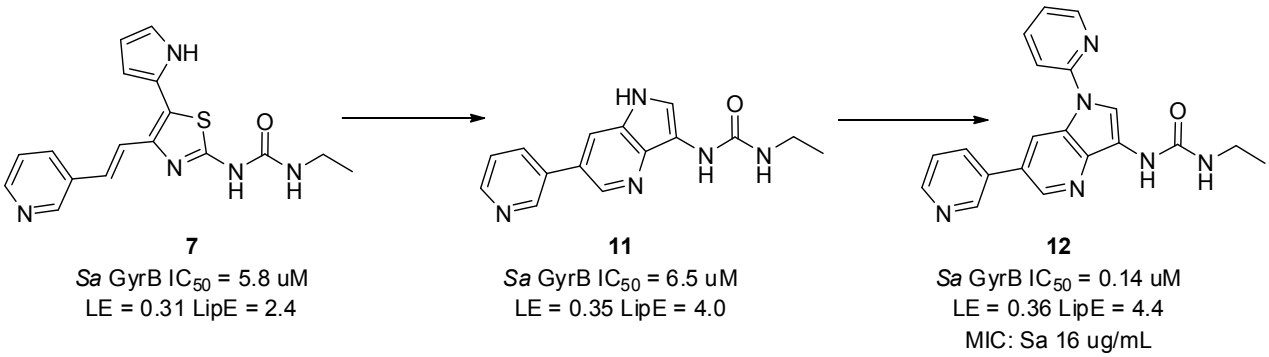

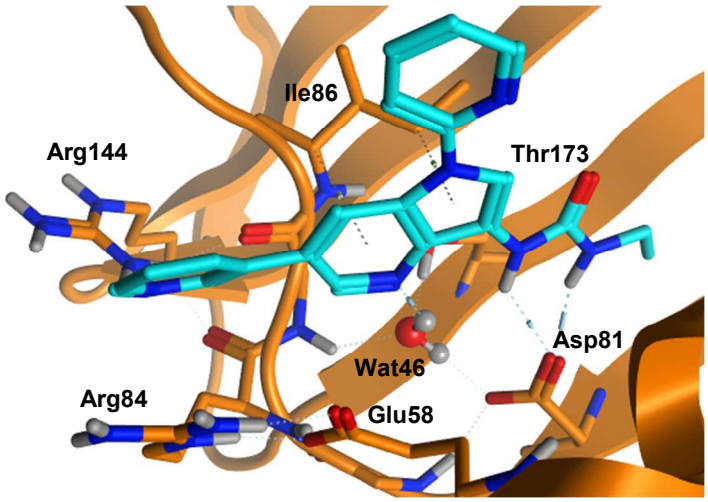

Figure 5. The evolution of azaindole **12** and its X-ray structure with 24 kDa *Sa* GyrB ATPase (PDB code 5D7C)

Scheme 1. The synthesis of aminothiazole **1f**[a]

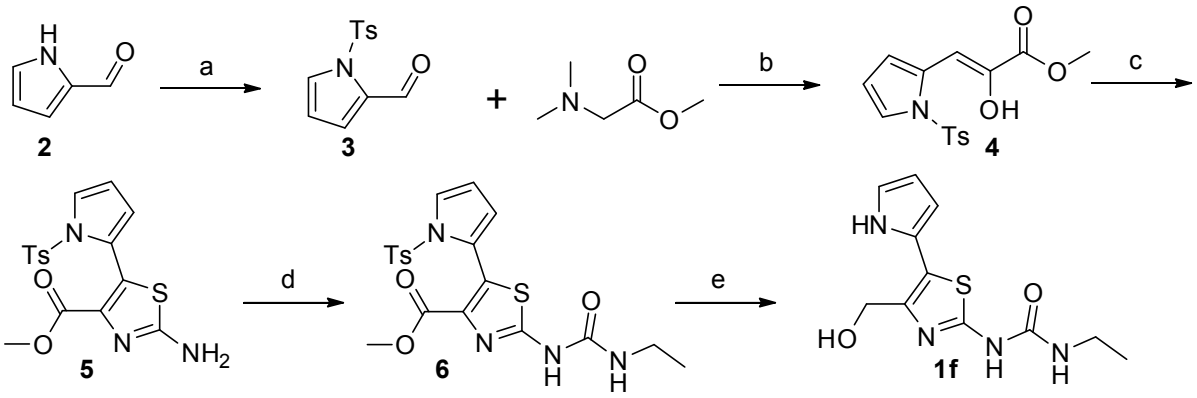

[a]Reaction conditions: a) NaH, TsCl, THF, 82%; b) NaH, THF, 15%; c) thiourea, I_2, dioxane, 28%; d) EtNCO, THF, 67%; e) $LiAlH_4$, THF, 8%

Scheme 2. Representative synthesis of azaindole urea analogs[a]

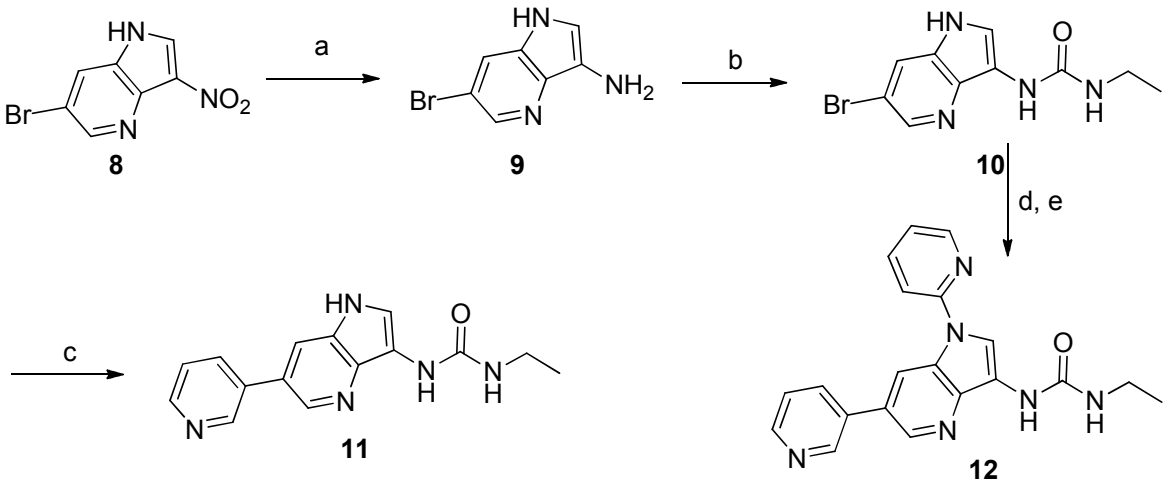

[a]Reaction conditons: a) Fe, NH_4Cl, EtOH, H_2O; b) ethyl isocyanate, THF, 75% over 2 steps, ; c) pyridin-3-ylboronic acid, $Pd(dppf)Cl_2$, Na_2CO_3 aq, 1,4-dioxane, 66%; d) 2-fluoropyridine, Cs_2CO_3, NMP, 43%; e) pyridin-3-ylboronic acid, $Pd(dppf)Cl_2$, Na_2CO_3 aq, 1,4-dioxane, 63%.

Table 1. Enzymatic and *in vitro* Antibacterial Activities of Azaindole Analogs: N1 Aryl SAR (MICs; µg/mL)

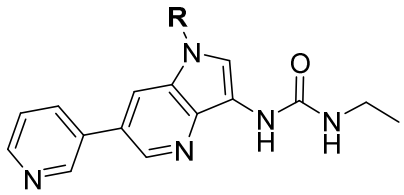

Cmpd	R	*Sa* GyrB ATPase IC50(uM)	MIC (ug/mL)					
			*Sa*42 MSSA	*Sa*1118 MRSA	*Sa*1721 MRSA Cipro^R	*S. Pneum.*	*E. Faecium*	*E. Faecalis*

11	H	6.50	>32	>32	>32	>32	>32	>32
12	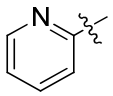	0.14	16	16	ND	8	8	8
13	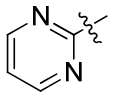	<0.079	8	8	16	4	8	2
14	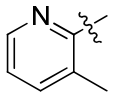	1.9	>32	>32	>32	>32	>32	>32
15	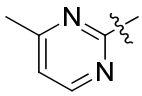	0.14	>32	>32	>32	4	2	1
16	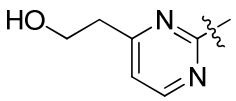	0.009	32	32	32	8	16	ND[a]
17	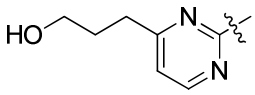	0.042	32	32	32	4	4	0.5
18	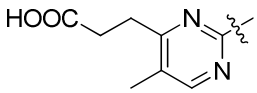	0.048	>32	>32	>32	1	>32	ND
19	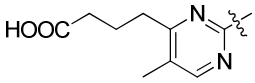	0.015	8	8	8	0.5	8	ND
20	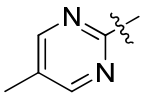	0.064	4	4	4	4	4	1
21	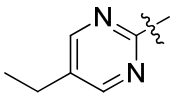	0.046	16	16	16	16	16	8
22	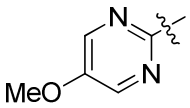	0.143	4	8	8	4	8	1
23	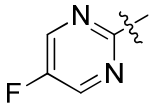	0.127	32	32	>32	32	32	32
24	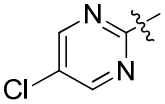	0.092	2	4	4	2	2	0.5
25	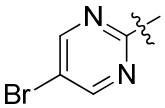	0.128	1	2	2	1	2	0.25

26	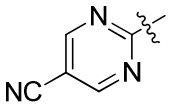	0.018	>32	>32	>32	>32	>32	>32
27	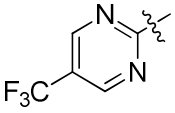	>100	>32	>32	>32	>32	>32	>32

[a]ND = Not Determined.

Table 2. Enzymatic Activities of Azaindole Analogs: N-nonaryl Substitutions

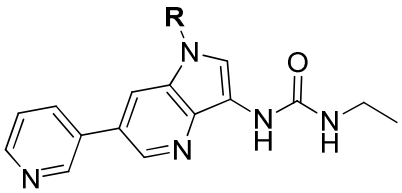

Cmpd	R	*Sa* GyrB ATPase IC_{50}(uM)	Cmpd	R	*Sa* GyrB ATPase IC_{50}(uM)
11	H	6.5	**33**	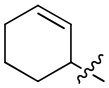	0.24
28	Me	1.8	**34**	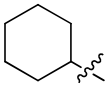	0.35
29	Bn	3.2	**35**	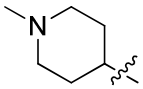	6.42
30	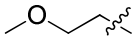	2.4	**36**	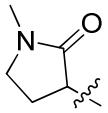	5.29
31	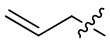	0.43	**37**	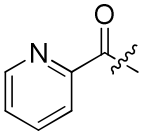	1.13
32	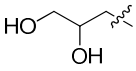	1.22	**38**	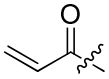	0.28

Table 3. Enzymatic and *in vitro* Antibacterial Activities of Azaindole Analogs: C6 Aryl SAR (MICs; µg/mL)

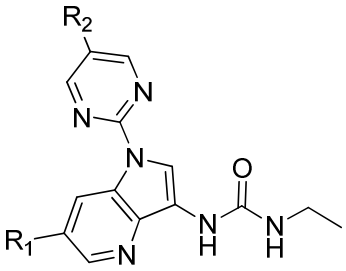

Cmpd	R^1	R^2	*Sa* GyrB ATPase IC50(uM)	MIC (ug/mL)					
				*Sa*42 MSSA	*Sa*1118 MRSA	*Sa*1721 MRSA Cipro^R	*S. Pneum.*	*E. Faecium*	*E. Faecalis*
12	3-Pyridyl	H	<0.079	8	8	16	4	8	2
39	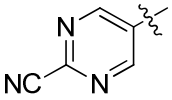	Cl	0.025	>32	>32	>32	>32	>32	>32
40	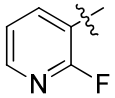	Cl	6.06	>32	>32	>32	>32	>32	>32
41	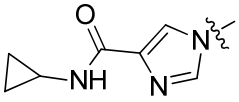	H	0.010	4	4	4	2	8	ND[a]
42	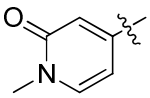	H	0.012	2	2	4	2	4	ND
43	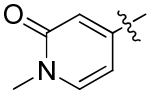	Me	0.013	>32	>32	>32	4	>32	0.5
44	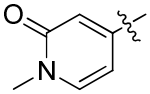	Cl	0.262	1	1	2	1	2	ND
45	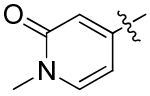	Et	0.071	1	1	1	0.25	0.25	ND

46	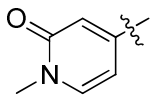	Br	0.094	1	1	1	1	1	ND
47	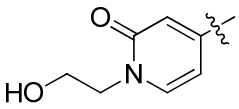	Br	0.008	8	8	8	8	8	ND

[a]ND = Not Determined.

AUTHOR INFORMATION

Corresponding Author

*Email: jackzhang49@yahoo.com. Phone: (781)640-2333

ACKNOWLEDGMENT

We would like to thank Dr. Ole Andersen and Dr. John Barker at Evotec AG for the crystallographic work, and Dr. Hongwu Gao's team in Chempartner for analog synthesis.

ABBREVIATIONS

GyrA, gyrase A; GyrB, gyrase B; SAR, structure activity relationship; MIC, minimum inhibitory concentration; ADME, absorption, distribution, metabolism and excretion; *MRSA*, methicillin-resistant *staphylococcus aureus*; *MSSA*, methicillin-susceptible *staphylococcus aureus; Sa*, *staphylococcus aureus*; *S. Pneum.*, *Streptococcus pneumonia; E. faecalis, Enterococcus faecalis; E. faecium, Enterococcus faecium*.

REFERENCES

(1) Bisacchi, G. S.; Manchester, J. I. A new-class antibacterial - almost. Lessons in drug discovery and development: a critical analysis of more than 50 years of effort toward ATPase inhibitors of DNA gyrase and topoisomerase IV. *ACS Infect. Dis.* **2015**, *1*, 4-41.

(2) Tomašić, T.; Mašič, L. P. Prospects for developing new antibacterials targeting bacterial type IIA topoisomerases. *Curr. Top. Med. Chem.* **2014**, *14*, 130–51.

(3) Oblak, M.; Kotnik, M.; Solmajer, T. Discovery and development of ATPase inhibitors of DNA gyrase as antibacterial agents. *Curr. Med. Chem.* **2007**, *14(19)*, 2033-47.

(4) Collin, F.; Karkare, S.; Maxwell, A. Exploiting bacterial DNA gyrase as a drug target: current state and perspectives. *Appl. Microbiol. Biotechnol.* **2011**, *92(3)*, 479–497.

(5) Tari, L. W.; Li, X.; Trzoss, M.; Bensen, D. C.; Chen, Z.; Lam, T.; Zhang, J.; Lee, S. J.; Hough, G.; Phillipson, D.; Akers-Rodriguez, S.; Cunningham, M. L.; Kwan, B. P.; Nelson, K. J.; Castellano, A.; Locke, J. B.; Brown-Driver, V.; Murphy, T. M.; Ong, V. S.; Pillar, C. M.; Shinabarger, D. L.; Nix, J.; Lightstone, F. C.; Wong, S. E.; Nguyen, T. B.; Shaw, K. J.; Finn, J. Tricyclic GyrB/ParE (TriBE) inhibitors: a new class of broad-spectrum dual-targeting antibacterial agents. *PLoS One* **2013**, *8(12)*, 1–13.

(6) Ronkin, S. M.; Badia, M.; Bellon, S.; Grillot, A. L.; Gross, C. H.; Grossman, T. H.; Mani, N.; Parsons, J. D.; Stamos, D.; Trudeau, M.; Wei, Y.; Charifson, P. S. Discovery of pyrazolthiazoles as novel and potent inhibitors of bacterial gyrase. *Bioorganic Med. Chem. Lett.* **2010**, *20*, 2828–2831.

(7) Charifson, P. S.; Grillot, A.-L.; Grossman, T. H.; Parsons, J. D.; Badia, M.; Bellon, S.; Deininger, D. D.; Drumm, J. E.; Gross, C. H.; LeTiran, A.; Liao, Y.; Mani, N.; Nicolau, D. P.; Perola, E.; Ronkin, S.; Shannon, D.; Swenson, L. L.; Tang, Q.; Tessier, P. R.; Tian, S.-K.; Trudeau, M.; Wang, T.; Wei, Y.; Zhang, H.; Stamos, D. Novel dual-targeting benzimidazole urea inhibitors of DNA gyrase and topoisomerase IV possessing potent antibacterial activity: intelligent design and evolution through the judicious use of structure-guided design and structure-activity relationships. *J. Med. Chem.* **2008**, *51(17)*, 5243-5263.

(8) Lewis, R. J.; Singh, O. M.; Smith, C. V; Skarzynski, T.; Maxwell, a; Wonacott, a J.; Wigley, D. B. The nature of inhibition of DNA gyrase by the coumarins and the cyclothialidines revealed by X-ray crystallography. *EMBO J.* **1996**, *15*, 1412–1420.

(9) Angehrn, P.; Goetschi, E.; Gmuender, H.; Hebeisen, P.; Hennig, M.; Kuhn, B.; Luebbers, T.; Reindl, P.; Ricklin, F.; Schmitt-Hoffmann, A. A new DNA gyrase inhibitor subclass of the cyclothialidine family based on a bicyclic dilactam-lactone scaffold: synthesis and antibacterial properties. *J. Med. Chem.* **2011**, *54(7)*, 2207–2224.

(10) Dumas, J.; Sherer, B. (2-pyridin-3-ylimidazo[1,2-b]pyridazin-6-yl) urea derivatives as antibacterial agents. Int. Pat. Appl. WO2009027733 A1.

(11) Basarab, G.; Hill, P.; Zhou, F. Piperidine compounds and uses thereof. Int. Pat. Appl. WO2008152418 A1.

(12) Illingworth, R.N.; Uria-Nickelsen, M.; Bryant, J.; Eakin, A.E. Presented at the 48th Interscience Conference on Antimicrobial Agents, Washington D.C., 2008, Poster F1-2028.

(13) Starr, J. T., Sciotti, R. J.; Hanna, D. L., Huband, M. D., Mullins, L. M., Cai, H., Gage, J. W., Lockard, M., Rauckhorst, M. R., Owen, R. M., Lall, M. S., Tomilo, M., Chen, H., McCurdy, S. P., Barbachyn, M. R. 5-(2-Pyrimidinyl)-imidazo[1,2-a]pyridines are antibacterial agents targeting the ATPase domains of DNA gyrase and topoisomerase IV. *Bioorg. Med. Chem. Lett.,* **2009**, *19(18)*, 5302-5306.

(14) 6-Bromo-3-nitro-1H-pyrrolo[3,2-b]pyridine was purchased from Sinova Product List.

(15) The detailed SAR studies will be reported in a future publication.

EXPERIMENTAL SECTION

General Procedures. All common solvents and chemicals were used as purchased without further purification. 6-Bromo-3-nitro-1H-pyrrolo[3,2-b]pyridine **8** was purchased from Sinova Product List. The progress of all reactions was monitored on Aldrich precoated silica gel plates (with fluorescence indicator UV254) using ethyl acetate/n-hexane or methanol/dichloromethane as solvent system, and by a Waters UPLC-MS with model number C10UPB090A. Column chromatography was performed with Aldrich silica gel 60 (230−400 mesh ASTM) with the solvent mixtures specified in the corresponding experiment. Purity of all final compounds was 95% or higher. Spots were visualized by irradiation with ultraviolet light (254 nm). Proton (1H) NMR spectra were recorded on Bruker Avance 500 or 300 MHz using solvents as indicated in the experimental section. Chemical shifts are given in parts per million (ppm) (δ relative to residual solvent peak for ^{1}H).

1-Tosyl-1*H*-pyrrole-2-carbaldehyde (3) To a solution of 1*H*-pyrrole-2-carbaldehyde **2** (5.0 g, 52.6 mmol) in THF (80 mL) was added NaH (2.31 g, 57.8 mmol) at 0^{o}C. After stirring at this temperature for 30 minutes, tosyl chloride (10.52 g, 55.2 mmol) in 20 mL THF was added drop wise. The reaction mixture was stirred at 0^{o}C for 2 hours, then diluted with ethyl acetate (200 mL). The organic phase was washed with water (100 mL), brine (50 mL), dried over Na_2SO_4 and evaporated *in vacuo*. The residue was purified by silica gel column chromatography eluting with 5% ethyl acetate in petroleum ether to give the title compound **3** (11 g, 82%) as a white solid. ^{1}H-NMR (400 MHz, $CDCl_3$): δ 2.42 (s, 3H), 6.40 (t, *J*=3.6 Hz, 1H), 7.16 (m, 1H), 7.32 (d, *J*=8.0 Hz, 2H), 7.62 (m, 1H), 7.82 (d, *J*=8.0 Hz, 2H) 9.97 (s, 1H).

(E)-Methyl 2-hydroxy-3-(1-tosyl-1*H*-pyrrol-2-yl)acrylate (4) To a 0^{o}C solution of NaH (2.88g, 72 mmol) in THF (60 mL) was added a solution of 1-tosyl-1*H*-pyrrole-2-carbaldehyde **3**

(8.98g, 36 mmol) and methyl 2-(*N, N*-dimethylamino)acetate (12.66 g, 108 mmol) in THF (60 mL). The mixture was then warmed up and stirred at room temperature for 4 hours. It was then diluted with ethyl acetate and water. The organic phase was washed with 1 N HCl (100mL), brine (50 mL), dried over Na_2SO_4, filtered and concentrated *in vacuo*. The residue was purified by silica gel column chromatography eluting with 10% ethyl acetate in petroleum ether to give the title compound **4** (2 g, 15%) as a white solid. ^{1}H-NMR (400MHz, DMSO-d^6): δ 2.36 (s, 3H), 3.82 (s, 3H), 6.44 (t, *J*=3.2 Hz, 1H), 6.93 (m, 1H), 7.03 (s, 1H), 7.44(d, *J*=8.0Hz, 2H), 7.49(m, 1H), 7.71 (d, *J*=8.0 Hz, 2H), 9.79 (s, 1H).

Methyl 2-amino-5-(1-tosyl-1*H*-pyrrol-2-yl)thiazole-4-carboxylate (5) A mixture of (*E*)-methyl 2-hydroxy-3-(1-tosyl-1*H*-pyrrol-2-yl)acrylate **4** (1.8 g, 5.6 mmol), thiourea (0.85 g, 11.2 mmol) and iodine (1.42 g, 5.6 mmol) in 150 mL 1, 4-dioxane was refluxed for 24 hours. The mixture was cooled down and diluted with ethyl acetate, washed with water, and brine. The organic phase was dried over Na_2SO_4, filtered and concentrated *in vacuo*. The residue was purified by silica gel column chromatography eluting with 1% methanol in dichloromethane to give the title compound **5** (0.6 g, 28%) ^{1}H-NMR (400MHz, $CDCl_3$): δ 2.39 (s, 3H), 3.44 (s, 3H), 5.46 (s, 2H), 6.32 (m, 2H), 7.22(d, *J*=8.0Hz, 2H), 7.50(m, 1H), 7.51 (d, *J*=8.0 Hz, 2H).

Methyl 2-(3-ethylureido)-5-(1-tosyl-1*H*-pyrrol-2-yl)thiazole-4-carboxylate (6) To a solution of methyl 2-amino-5-(1-tosyl-1*H*-pyrrol-2-yl)thiazole-4-carboxylate **5** (0.51 g, 1.35 mmol) in THF (100 mL) was added ethyl isocyanate (1.92 g, 27 mmol) at room temperature. The mixture was then refluxed for 3 days. The mixture was concentrated *in vacuo* and purified by silica gel column chromatography eluting with 2% methanol in dichloromethane to give the title compound **6** (0.4 g, 67%). H-NMR (400MHz, DMSO-d^6): δ 1.07 (t, *J*=7.2Hz, 3H), 2.35 (s, 3H),

3.16 (m, 2H), 3.41(s, 3H) 6.37 (m, 1H), 6.41 (m, 1H), 6.83(br, 1H), 7.33(d, *J*=8.4 Hz, 2H), 7.42(d, *J*=8.4 Hz, 2H), 7.58(m, 1H), 11.08(br, 1H). MS (EI$^+$, *m/z*): 449 $[M+H]^+$.

1-Ethyl-3-(4-(hydroxymethyl)-5-(1*H*-pyrrol-2-yl)thiazol-2-yl)urea (1f) To a solution of methyl 2-(3-ethylureido)-5-(1-tosyl-1*H*-pyrrol-2-yl)thiazole-4-carboxylate **6** (3.0 g, 6.7 mmol) in THF (450 mL) was added $LiAlH_4$ (1.27 g, 33.4 mmol) at 0^{o}C. The mixture was slowly warmed up to room temperature and stirred overnight. The mixture was carefully quenched by $Na_2SO_4 \cdot 10H_2O$ (5 g), filtered and concentrated *in vacuo*. The residue was purified by silica gel chromatography eluting with 3% methanol in dichloromethane to give the title compound **1f** (0.15 g, 8%). ^{1}H-NMR (400MHz, DMSO-d^6): δ 1.06 (t, *J* = 7.2Hz, 3H), 3.15-3.16 (m, 2H), 4.39(s, 2H), 5.23-5.25 (br, 1H), 6.10-6.12 (m, 1H), 6.20-6.22 (m, 1H), 6.53-6.55 (br, 1H), 6.82-6.84 (m, 1H), 10.29-10.30 (br, 1H), 10.96 (s, 1H). MS (EI$^+$, *m/z*): 267 $[M+H]^+$.

1-(6-Bromo-1*H*-pyrrolo[3,2-b]pyridin-3-yl)-3-ethylurea (10) To a solution of 6-bromo-3-nitro-1*H*-pyrrolo[3,2-b]pyridine **8** (1.21 g, 5.0 mmol) in water (20 mL) and ethanol (300 mL) was added NH_4Cl (1.34 g, 25.0 mmol) and iron powder (1.40 g, 25.0 mmol) in two portions. The mixture was heated to 80^{o}C for 2 h and cooled to room temperature, filtered through celite. The filtrate was concentrated to give the crude product **9** (1.06 g, 100%) as a dark solid, which was taken to the next step without further purification. MS (EI$^+$, *m/z*): 213 $[M+H]^+$.

To a suspension of the 6-bromo-1*H*-pyrrolo[3,2-b]pyridin-3-amine **9** (1.06 g, 5 mmol) in THF (60 mL) was added ethyl isocyanate (1.8 g, 25.0 mmol). The reaction mixture was heated at 70^{o}C for 1.5 hours and then concentrated. The residue was purified by silica gel column chromatography eluting with 33% ethyl acetate in hexane to afford the title compound **10** (1.06 g, 75% over 2 steps) as an off-white solid. ^{1}H-NMR (500 MHz, DMSO-*d*^{6}): δ 10.92 (s, 1H), 8.37

(s, 1H), 8.33 (s, 1H), 7.95 (s, 1H), 7.75 (s, 1H), 6.42-6.44 (m, 1H), 3.12-3.16 (m, 2H), 1.05 (t, *J* = 6.0 Hz, 3H). MS (EI^+, *m/z*): 283 $[M+H]^+$.

1-Ethyl-3-(6-(pyridin-3-yl)-1*H*-pyrrolo[3,2-b]pyridin-3-yl)urea (11) A mixture of 1-(6-bromo-1*H*-pyrrolo[3,2-b]pyridin-3-yl)-3-ethylurea **10** (120 mg, 0.426 mmol), pyridin-3-yl boronic acid (105 mg, 0.85 mmol), $Pd(dppf)Cl_2$ (13 mg, 0.002 mmol) and aqeous Na_2CO_3 (0.6 mL, 1.21 mmol, 2 M) in 1,4-dioxane (5.0 mL) was heated at 130 ^oC for 30 minutes in the microwave reactor under N_2 atmosphere. The reaction mixture was purified by reverse phase HPLC directly to give the title compound **11** (77 mg, 66%) as an off-white solid. ^1H-NMR (500 MHz, DMSO-d^6): δ 11.83 (s, 1H), 9.12 (s, 1H), 8.82 (s, 1H), 8.72 (s, 1H), 8.54 (s, 1H), 8.43 (s, 1H), 7.97 (d, *J* = 2.0 Hz, 1H), 7.72-7.75 (m, 1H), 6.58-6.59 (m, 1H), 3.16-3.18 (m, 2H), 1.06-1.08 (m, 3H). MS (EI^+, *m/z*): 282.1$[M+H]^+$.

1-ethyl-3-(1-(pyridin-2-yl)-6-(pyridin-3-yl)-1*H*-pyrrolo[3,2-b]pyridin-3-yl)urea (12) To a mixture of 1-(6-bromo-1*H*-pyrrolo[3,2-b]pyridin-3-yl)-3-ethylurea **10** (200 mg, 0.71 mmol) in *N*-methylpyrrolidinone (7.5 mL) was added Cs_2CO_3 (1.16 g, 3.55 mmol) and 2-fluoropyridine (138 mg, 1.42 mmol). The mixture was heated at 150 ^oC for 30 minutes in a microwave reactor and cooled to room temperature and treated with water (40 mL). The resulting precipitates were collected and dried *in vacuo* to give the crude 1-(6-bromo-1-(pyridin-2-yl)-1*H*-pyrrolo[3,2-b]pyridin-3-yl)-3-ethylurea (190 mg, 43%) as an off-white solid, which was taken to the next step without further purification. MS (EI^+, *m/z*): 360.1$[M+H]^+$.

A mixture of 1-(6-bromo-1-(pyridin-2-yl)-1*H*-pyrrolo[3,2-b]pyridin-3-yl)-3-ethylurea (160 mg, 0.446 mmol), pyridin-3-yl boronic acid (110 mg, 0.89 mmol), $Pd(dppf)Cl_2$ (13 mg, 0.002 mmol) and aqueous Na_2CO_3 (0.7 mL, 1.34 mmol, 2 M) in 1,4-dioxane (2.0 mL) was heated at 130 ^oC

for 30 minutes in a microwave reactor under N_2 atmosphere. The reaction mixture was purified by reverse phase HPLC directly to give the title compound **12** (120 mg, 63%) as an off-white solid. ^{1}H-NMR (500 MHz, DMSO-d^6): δ 9.06-9.28 (m, 2H), 8.52-8.92 (m, 6H), 7.78-8.05 (m, 3H), 7.30-7.36 (m, 1H), 6.70-6.72 (m, 1H), 3.20-3.22 (m, 2H), 1.12 (t, J = 7.0 Hz, 3H). MS (EI$^+$, *m/z*): 329.1[M+H]$^+$.

1-Ethyl-3-(6-(pyridin-3-yl)-1-(pyrimidin-2-yl)-1*H*-pyrrolo[3,2-b]pyridin-3-yl)urea (13) ^{1}H-NMR (500 MHz, DMSO-d^6): δ 9.28 (s, 1H), 9.20 (s, 1H), 8.78-8.88 (m, 6H), 8.57 (d, J = 8.0 Hz, 1H), 7.87 (t, J = 5.5 Hz, 1H), 7.34 (t, J = 4.5 Hz, 1H), 6.70 (s, 1H), 3.18 (m, 2H), 1.10 (t, J = 7.0 Hz, 3H). MS (EI$^+$, *m/z*): 360.2 [M+H]$^+$.

1-Ethyl-3-(1-(3-methylpyridin-2-yl)-6-(pyridin-3-yl)-1*H*-pyrrolo[3,2-b]pyridin-3-yl)urea (14) ^{1}H-NMR (500 MHz, DMSO-d^6): δ 8.95 (s, 1H), 8.77 (s, 1H), 8.69 (s, 1H), 8.58 (s, 1H), 8.45 (s, 1H), 8.15 (s, 1H), 8.07 (s, 1H), 8.01 (s, 1H), 7.95 (d, J = 7.5 Hz, 1H), 7.42-7.50 (m, 2H), 6.59 (t, J = 5.5 Hz, 1H), 3.16-3.18 (m, 2H), 1.09 (t, J = 7.5 Hz, 3H). MS (EI$^+$, *m/z*): 373.2 [M+H]$^+$.

1-Ethyl-3-(1-(4-methylpyrimidin-2-yl)-6-(pyridin-3-yl)-1*H*-pyrrolo[3,2-b]pyridin-3-yl)urea (15) ^{1}H-NMR (400 MHz, DMSO-d^6): δ 9.19 (dd, J = 9.6 Hz, J = 1.6Hz, 2H), 8.70-8.86 (m, 6H), 8.56 (d, J = 2.0 Hz, 1H), 7.86 (dd, J = 8.0, J = 5.2Hz), 6.70 (s, 1H), 3.18 (m, 2H), 2.30 (s, 3H), 1.10 (t, J = 6.8 Hz, 3H). MS (EI$^+$, *m/z*): 373.1 [M+H]$^+$.

1-Ethyl-3-(1-(4-(2-hydroxyethyl)pyrimidin-2-yl)-6-(pyridin-3-yl)-1*H*-pyrrolo[3,2-b]pyridin-3-yl)urea (16) ^{1}H-NMR (500 MHz, DMSO-d^6): δ 9.28 (d, J = 2.0 Hz, 2H), 9.01 (d, J = 2.0 Hz, 1H), 8.64-8.84 (m, 5H), 8.21 (t, J = 7.0 Hz, 1H), 7.56-7.59 (m, 1H), 7.23 (s, 1H), 6.71 (s, 1H),

3.91 (t, *J* = 6.0 Hz, 2H), 3.17-3.19 (m, 2H), 2.99 (t, *J* = 6.0 Hz, 2H), 1.10(t, *J* = 7.0 Hz, 3H). MS (EI$^+$, *m/z*): 404.1 [M+H]$^+$.

1-Ethyl-3-(1-(4-(3-hydroxypropyl)pyrimidin-2-yl)-6-(pyridin-3-yl)-1*H*-pyrrolo[3,2-b]pyridin-3-yl)urea (17) ^{1}H-NMR (500 MHz, DMSO-*d*^{6}): δ 9.31 (d, *J* = 2.0 Hz, 1H), 9.12 (d, *J* = 2.0 Hz, 1H), 8.71-8.87 (m, 5H), 8.42 (d, *J* = 7.0 Hz, 1H), 7.73 (t, *J* = 5.5 Hz, 1H), 7.23 (d, *J* = 5.0 Hz, 1H), 6.70 (s, 1H), 3.52 (t, *J* = 6.5 Hz, 2H), 3.17-3.19 (m, 2H), 2.88 (t, *J* = 8.0 Hz, 2H), 1.94-2.00 (m, 2H), 1.10(t, *J* = 7.5 Hz, 3H). MS (EI$^+$, *m/z*): 418.2 [M+H]$^+$.

3-(2-(3-(3-Ethylureido)-6-(pyridin-3-yl)-1*H*-pyrrolo[3,2-b]pyridin-1-yl)pyrimidin-4-yl)propanoic acid (18) ^{1}H-NMR (500 MHz, DMSO-*d*^{6}): δ 9.24 (s, 1H), 9.05 (s, 1H), 8.76-8.82 (m, 3H), 8.73 (s, 1H), 8.63 (d, *J* = 4.0 Hz, 1H), 8.53 (s, 1H), 8.26 (d, *J* = 9.0 Hz, 1H), 7.55 (dd, *J* = 7.5 Hz, *J* = 5.0 Hz, 1H), 6.69 (d, *J* = 5.5 Hz, 1H), 3.15-3.20 (m, 2H), 3.03-3.07 (m, 2H), 2.88 (m, 2H), 2.28 (s, 3H), 1.09 (t, *J* = 7.0 Hz, 3H). MS (EI$^+$, *m/z*): 445.2 [M+H]$^+$.

4-(2-(3-(3-ethylureido)-6-(pyridin-3-yl)-1*H*-pyrrolo[3,2-b]pyridin-1-yl)pyrimidin-4-yl)butanoic acid (19) ^{1}H-NMR (400 MHz, DMSO-*d*^{6}): δ 9.15 (s, 1H), 8.97 (s, 1H), 8.60-8.77 (m, 4H), 8.43 (s, 1H), 8.14 (d, *J* = 8.0 Hz, 1H), 7.54 (dd, *J* = 8.0 Hz, *J* = 5.2 Hz, 1H), 6.67 (t, *J* = 5.2 Hz, 1H), 3.13-3.23 (m, 2H), 2.78 (t, *J* = 7.2 Hz, 2H), 2.35 (t, *J* = 7.2 Hz, 2H), 2.19 (s, 3H), 2.03 (t, *J* = 7.2 Hz, 2H), 1.09 (t, *J* = 7.2 Hz, 3H). MS (EI$^+$, *m/z*): 459.2 [M+H]$^+$.

1-Ethyl-3-(1-(5-methylpyrimidin-2-yl)-6-(pyridin-3-yl)-1*H*-pyrrolo[3,2-b]pyridin-3-yl)urea (20) ^{1}H-NMR (400 MHz, DMSO-*d*^{6}): δ 9.29 (d, *J* = 2.0 Hz, 1H), 9.20 (d, *J* = 2.0 Hz, 1H), 8.87 (d, *J* = 2.0 Hz, 1H), 8.77-8.81 (m, 3H), 8.70 (d, *J* = 2.8 Hz, 1H), 8.58 (d, *J* = 8.4 Hz, 1H), 7.88

(dd, *J* = 8.0 Hz, 5.6 Hz, 1H), 7.22 (d, *J* = 9.2 Hz, 1H), 6.70 (s, 1H), 3.18 (d, *J* = 6.0 Hz, 2H), 2.58 (s, 3H), 1.10 (t, *J* = 7.2 Hz, 3H). MS (EI$^+$, *m/z*): 373.1 $[M+H]^+$.

1-Ethyl-3-(1-(5-ethylpyrimidin-2-yl)-6-(pyridin-3-yl)-1*H*-pyrrolo[3,2-b]pyridin-3-yl)urea (21) ^{1}H-NMR (500 MHz, DMSO-d^6): δ 9.20 (d, *J* = 1.0 Hz, 1H), 9.00 (d, *J* = 2.5 Hz, 1H), 8.73-8.82 (m, 5H), 8.64 (t, *J* = 4.0 Hz, 1H), 7.56-7.58 (m, 1H), 6.68 (t, *J* = 5.0 Hz, 1H), 3.17-3.21 (m, 2H), 2.63-2.68 (m, 2H), 1.25(t, *J* = 7.5 Hz, 3H), 1.10(t, *J* = 7.0 Hz, 3H). MS (EI$^+$, *m/z*): 388.2 $[M+H]^+$.

1-Ethyl-3-(1-(5-methoxypyrimidin-2-yl)-6-(pyridin-3-yl)-1*H*-pyrrolo[3,2-b]pyridin-3-yl)urea (22) ^{1}H-NMR (500 MHz, DMSO-d^6): δ 9.19 (d, *J* = 1.5 Hz, 1H), 9.11 (s, 1H), 8.84 (d, *J* = 2.0 Hz, 1H), 8.78 (s, 1H), 8.72-8.74 (m, 2H), 8.67 (s, 2H), 8.42 (s, 1H), 7.75 (s, 1H), 6.68 (s, 1H), 3.98 (s, 3H), 3.17 (m, 2H), 1.09 (t, *J* = 7.0 Hz, 3H). MS (EI$^+$, *m/z*): 390.2 $[M+H]^+$.

1-Ethyl-3-(1-(5-fluoropyrimidin-2-yl)-6-(pyridin-3-yl)-1*H*-pyrrolo[3,2-b]pyridin-3-yl)urea (23) ^{1}H-NMR (500 MHz, DMSO-d^6): δ 9.15-9.17 (m, 2H), 8.97 (s, 2H), 8.87 (d, *J* = 2.0 Hz, 1H), 8.82 (s, 1H), 8.77 (s, 2H), 8.71 (s, 1H), 8.49 (d, *J* = 7.5 Hz, 1H), 7.80 (s, 1H), 6.70 (s, 1H), 3.17 (m, 2H), 1.09(t, *J* = 7.0 Hz, 3H). MS (EI$^+$, *m/z*): 378.2 $[M+H]^+$.

1-(1-(5-Chloropyrimidin-2-yl)-6-(pyridin-3-yl)-1*H*-pyrrolo[3,2-b]pyridin-3-yl)-3-ethylurea (24) ^{1}H-NMR (500 MHz, DMSO-d^6): δ 9.12-9.16 (m, 2H), 8.96 (s, 2H), 8.87 (d, *J* = 2.0 Hz, 1H), 8.84 (s, 1H), 8.75-8.76 (m, 2H), 8.68 (s, 1H), 8.44-8.46 (m, 1H), 7.77-7.79 (m, 1H), 6.70 (s, 1H), 3.17 (m, 2H), 1.09(t, *J* = 7.0 Hz, 3H). MS (EI$^+$, *m/z*): 394.1 $[M+H]^+$.

1-(1-(5-Bromopyrimidin-2-yl)-6-(pyridin-3-yl)-1*H*-pyrrolo[3,2-b]pyridin-3-yl)-3-ethylurea (25) ^{1}H-NMR (500 MHz, DMSO-d^6): δ 9.09 (s, 1H), 8.99 (s, 3H), 8.80-8.81 (m, 2H), 8.63-8.65 (m, 2H), 8.18 (d, J = 7.5 Hz, 1H), 7.51 (s, 1H), 6.70 (s, 1H), 3.18-3.19 (m, 2H), 1.09(t, J = 7.0 Hz, 3H). MS (EI$^+$, *m/z*): 438.0 $[M+H]^+$.

1-(1-(5-Cyanopyrimidin-2-yl)-6-(pyridin-3-yl)-1*H*-pyrrolo[3,2-b]pyridin-3-yl)-3-ethylurea (26) ^{1}H-NMR (500 MHz, DMSO-d^6): δ 9.29 (s, 2H), 9.15 (d, J = 2.0 Hz, 1H), 9.00 (s, 1H), 8.92 (s, 1H), 8.88 (d, J = 2.0 Hz, 1H), 8.67 (s, 2H), 8.20 (d, J = 8.0 Hz, 1H), 7.57-7.60 (m, 1H), 6.75 (t, J = 5.5 Hz, 1H), 3.17-3.19 (m, 2H), 1.09 (t, J = 7.0 Hz, 3H). MS (EI$^+$, *m/z*): 385.1 $[M+H]^+$.

1-Ethyl-3-(6-(pyridin-3-yl)-1-(5-(trifluoromethyl)pyrimidin-2-yl)-1*H*-pyrrolo[3,2-b]pyridin-3-yl)urea (27) ^{1}H NMR (300 MHz, DMSO-d^6) δ 9.24 (s, 2H), 9.19 (d, J = 2.0 Hz, 1H), 8.97 (s, 1H), 8.88 – 8.82 (m, 2H), 8.68 (s, 1H), 8.61 (d, J = 3.4 Hz, 1H), 8.17 (d, J = 8.4 Hz, 1H), 7.53 (dd, J = 8.1, 4.9 Hz, 1H), 6.70 (s, 1H), 3.19 – 3.09 (m, 2H), 1.04 (t, J = 7.2 Hz, 3H).

1-Ethyl-3-(1-methyl-6-(pyridin-3-yl)-1*H*-pyrrolo[3,2-b]pyridin-3-yl)urea (28) ^{1}H-NMR (500 MHz, DMSO-d^6): δ 9.29 (s, 1H), 9.05 (s, 1H), 8.94 (s, 1H), 8.88 (d, J = 5.0 Hz, 1H), 8.82 (d, J = 8.5 Hz, 1H), 8.02-8.06 (m, 2H), 4.10 (s, 3H), 3.32-3.34 (m, 4H), 1.21 (t, J = 7.0 Hz, 3H). MS (EI$^+$, *m/z*): 296.1 $[M+H]^+$.

1-(1-Benzyl-6-(pyridin-3-yl)-1*H*-pyrrolo[3,2-b]pyridin-3-yl)-3-ethylurea (29) ^{1}H-NMR (500 MHz, DMSO-d^6): δ 9.24 (s, 1H), 8.86 (s, 1H), 8.80 (d, J = 4.5 Hz, 1H), 8.75 (s, 1H), 8.64-8.66 (m, 2H), 8.05 (s, 1H), 7.88-7.90 (m, 1H), 7.30-7.31 (m, 5H), 6.60 (s, 1H), 5.55 (s, 2H), 3.31-3.34 (m, 2H), 1.07 (t, J = 7.0 Hz, 3H). MS (EI$^+$, *m/z*): 372.2 $[M+H]^+$.

1-Ethyl-3-(1-(2-methoxyethyl)-6-(pyridin-3-yl)-1*H*-pyrrolo[3,2-b]pyridin-3-yl)urea (30) ^{1}H-NMR (500 MHz, DMSO-d^6): δ 9.02 (d, J = 1.0 Hz, 1H), 8.65 (s, 1H), 8.58 (d, J = 5.0 Hz, 1H), 8.47 (s, 1H), 8.26 (s, 1H), 8.19 (d, J = 8.0 Hz, 1H), 7.85 (s, 1H), 7.51-7.54 (m, 1H), 6.50 (s, 1H), 4.37(t, J = 4.5 Hz, 2H), 3.65 (t, J = 4.5 Hz, 2H), 3.22 (s, 3H), 3.14 (t, J = 6.5 Hz, 3H), 1.07(t, J = 7.0 Hz, 3H). MS (EI$^+$, *m/z*): 340.2 [M+H]$^+$.

1-(1-Allyl-6-(pyridin-3-yl)-1*H*-pyrrolo[3,2-b]pyridin-3-yl)-3-ethylurea (31) ^{1}H-NMR (500 MHz, DMSO-d^6): δ 9.00 (s, 1H), 8.66 (d, J = 2.0 Hz, 1H), 8.58-8.59 (m, 1H), 8.50 (s, 1H), 8.23 (d, J = 2.0 Hz, 1H), 8.18 (d, J = 8.0 Hz, 1H), 7.82(s, 1H), 7.51-7.53 (m, 1H), 6.49 (s, 1H), 5.98-6.01 (m, 1H), 5.10-5.18 (m, 2H), 4.86 (d, J = 5.5 Hz, 2H), 3.12-3.15 (m, 2H), 1.06 (t, J = 6.0 Hz, 3H). MS (EI$^+$, *m/z*): 322.0 [M+H]$^+$.

1-(1-(2,3-Dihydroxypropyl)-6-(pyridin-3-yl)-1*H*-pyrrolo[3,2-b]pyridin-3-yl)-3-ethylurea (32) ^{1}H-NMR (500 MHz, DMSO-d^6): δ 9.00 (d, J = 2.0 Hz, 1H), 8.63 (d, J = 2.0 Hz, 1H), 8.58 (d, J = 4.5 Hz, 1H), 8.17-8.20 (m, 2H), 7.85 (s, 1H), 7.51-7.54 (m, 1H), 6.48 (t, J = 6.0 Hz, 1H), 4.99 (d, J = 5.0 Hz, 1H), 4.79 (t, J = 5.0 Hz, 1H), 4.28-4.32 (m, 1H), 4.10-4.15 (m, 1H), 3.78 (d, J = 4.5 Hz, 1H), 3.37 (s, 1H), 3.27-3.30 (m, 1H), 3.11-3.17 (m, 2H), 1.07 (t, J = 7.0 Hz, 3H). MS (EI$^+$, *m/z*): 356.1 [M+H]$^+$.

1-(1-(Cyclohex-2-en-1-yl)-6-(pyridin-3-yl)-1*H*-pyrrolo[3,2-b]pyridin-3-yl)-3-ethylurea (33) ^{1}H-NMR (500 MHz, DMSO-d^6): δ 9.14 (s, 1H), 8.76 (s, 1H), 8.69 (d, J = 3.0 Hz, 1H), 8.51-8.53 (m, 2H), 8.45 (d, J = 7.5 Hz, 1H), 7.88 (s, 1H), 7.71 (s, 1H), 6.53 (s, 1H), 6.16-6.18 (m, 1H), 5.78-5.80 (m, 1H), 5.35 (s, 1H), 3.22-3.30 (m, 2H), 2.07-2.20 (m, 2H), 1.71-1.73 (m, 3H), 1.06 (t, J = 7.0 Hz, 3H). MS (EI$^+$, *m/z*): 362.2 [M+H]$^+$.

1-(1-Cyclohexyl-6-(pyridin-3-yl)-1*H*-pyrrolo[3,2-b]pyridin-3-yl)-3-ethylurea (34) ^{1}H-NMR (500 MHz, DMSO-d^6): δ 9.03 (d, J = 2.0 Hz, 1H), 8.64 (d, J = 1.5 Hz, 1H), 8.58-8.59 (m, 1H), 8.46 (s, 1H), 8.33 (d, J = 1.5 Hz, 1H), 8.22 (d, J = 8.0 Hz, 1H), 7.91 (s, 1H),7.51-7.53 (m, 1H), 6.48 (s, 1H), 4.50 (s, 1H), 3.12-3.14 (m, 2H), 1.94-1.95 (m, 2H), 1.84-1.85 (m, 2H), 1.71-1.72 (m, 2H), 1.50-1.51 (m, 2H), 1.32-1.35 (m, 1H), 1.07 (t, J = 7.0 Hz, 3H). MS (EI^+, *m/z*): 364.3 $[M+H]^+$.

1-Ethyl-3-(1-(1-methylpiperidin-4-yl)-6-(pyridin-3-yl)-1*H*-pyrrolo[3,2-b]pyridin-3-yl)urea (35) MS (EI^+, *m/z*): 379.2 $[M+H]^+$.

1-Ethyl-3-(1-(1-methyl-2-oxopyrrolidin-3-yl)-6-(pyridin-3-yl)-1*H*-pyrrolo[3,2-b]pyridin-3-yl)urea (36) ^{1}H-NMR (500 MHz, DMSO-d^6): δ 9.00 (d, J = 2.0 Hz, 1H), 8.68 (d, J = 2.0 Hz, 1H), 8.59-8.60 (m, 1H), 8.55 (s, 1H), 8.18-8.22 (m, 2H), 7.72(s, 1H), 7.52-7.55 (m, 1H), 6.50-6.51 (m, 1H), 5.50-5.51 (m, 1H), 3.52-3.54 (m, 2H), 3.12-3.14 (m, 2H), 2.88 (s, 3H), 2.60-2.62 (m, 1H), 2.20-2.24 (m, 1H), 1.06 (t, J = 6.0 Hz, 3H). MS (EI^+, *m/z*): 379.3 $[M+H]^+$.

1-Ethyl-3-(1-picolinoyl-6-(pyridin-3-yl)-1*H*-pyrrolo[3,2-b]pyridin-3-yl)urea (37) ^{1}H-NMR (500 MHz, DMSO-d^6): δ 9.00 (s, 1H), 8.95 (s,1H), 8.82-8.85 (m, 2H), 8.65 (d, J = 1.5 Hz, 1H), 8.36 (s, 1H), 8.21 (d, J = 3.0 Hz, 1H), 8.14-8.17 (m, 1H), 8.07(s, 1H), 7.74-7.77 (m, 1H), 7.56-7.59 (m, 1H), 6.72-6.73 (m, 1H), 3.22-3.24 (m, 2H), 1.05 (t, J = 7.5 Hz, 3H). MS (EI^+, *m/z*): 387.1 $[M+H]^+$.

1-(1-Acryloyl-6-(pyridin-3-yl)-1*H*-pyrrolo[3,2-b]pyridin-3-yl)-3-ethylurea (38) ^{1}H-NMR (500 MHz, DMSO-d^6): δ 8.99 (d, J = 2.0 Hz, 1H), 8.86-8.91 (m, 3H), 8.64-8.66 (m, 1H), 8.30 (s, 1H), 8.20 (t, J = 6.0 Hz, 1H), 7.55-7.58 (m, 1H), 7.24-7.30 (m, 1H), 6.73 (s, 1H), 6.54-6.58 (m,

1H), 6.14-6.16 (m, 1H), 3.16-3.19 (m, 2H), 1.10 (t, *J* = 7.0 Hz, 3H). MS (EI$^+$, *m/z*): 336.1 $[M+H]^+$.

1-(1-(5-Chloropyrimidin-2-yl)-6-(2-cyanopyrimidin-5-yl)-1*H*-pyrrolo[3,2-b]pyridin-3-yl)-3-ethylurea (39) ^{1}H NMR (300 MHz, DMSO-*d*^{6}) δ 9.44 (s, 2H), 9.23 (d, *J* = 1.9 Hz, 1H), 8.94 (d, *J* = 2.0 Hz, 1H), 8.91 (s, 2H), 8.82 (s, 1H), 8.68 (s, 1H), 8.41 (s, 2H), 6.67 (s, 1H), 3.12 (m, 2H), 1.03 (t, *J* = 7.2 Hz, 3H). MS (EI$^+$, *m/z*): 420.6 $[M+H]^+$.

1-(1-(5-Chloropyrimidin-2-yl)-6-(2-fluoropyridin-3-yl)-1*H*-pyrrolo[3,2-b]pyridin-3-yl)-3-ethylurea (40) ^{1}H NMR (300 MHz, DMSO-*d*^{6}) δ 9.10 (t, *J* = 1.7 Hz, 1H), 8.95 (s, 2H), 8.84 (s, 1H), 8.73 – 8.68 (m, 2H), 8.35 – 8.30 (m, 1H), 8.26 (dd, *J* = 9.9, 2.2 Hz, 1H), 7.56 (ddd, *J* = 7.1, 4.8, 1.8 Hz, 1H), 6.70 (t, *J* = 5.5 Hz, 1H), 3.17 (dt, *J* = 12.6, 7.0 Hz, 2H), 1.09 (t, *J* = 7.2 Hz, 3H). MS (EI$^+$, *m/z*): 412.6 $[M+H]^+$.

N-Cyclopropyl-1-(3-(3-ethylureido)-1-(pyrimidin-2-yl)-1*H*-pyrrolo[3,2-b]pyridin-6-yl)-1H-imidazole-4-carboxamide (41) ^{1}HNMR (500 MHz, DMSO-*d*^{6}) δ 9.16 - 9.15 (m, 1H), 8.89 (d, *J* = 4.8 Hz, 2H), 8.86 - 8.84 (m, 2H), 8.77 (s, 1H), 8.40 (s, 1H), 8.30 (s, 1H), 8.15 - 8.14 (m, 1H), 7.36 (t, *J* = 4.8 Hz, 1H), 6.69-6.67 (m, 1H), 3.19 - 3.16 (m, 2H), 2.88 - 2.82 (m, 1H), 1.09 (t, *J* = 7.2 Hz, 3H), 0.71 - 0.61 (m, 4H). MS (EI$^+$, *m/z*): 432.2 $[M+H]^+$.

1-Ethyl-3-(6-(1-methyl-2-oxo-1,2-dihydropyridin-4-yl)-1-(pyrimidin-2-yl)-1*H*-pyrrolo[3,2-b]pyridin-3-yl)urea (42) ^{1}HNMR (500 MHz, DMSO-*d*^{6}) δ 9.21 - 9.20 (m, 1H), 8.89 (d, *J* = 4.8 Hz, 2H), 8.84 - 8.80 (m, 2H), 8.78 (s, 1H), 7.87 - 7.85 (m, 1H), 7.34 (t, *J* = 4.8 Hz, 1H), 6.82 - 6.78 (m, 1H), 6.73 - 6.67 (m, 2H), 3.49 (s, 3H), 3.19 - 3.16 (m, 2H), 1.09 (t, *J* = 7.2 Hz, 3H). MS (EI$^+$, *m/z*): 390.0 $[M+H]^+$.

1-Ethyl-3-(6-(1-methyl-2-oxo-1,2-dihydropyridin-4-yl)-1-(5-methylpyrimidin-2-yl)-1*H*-pyrrolo[3,2-b]pyridin-3-yl)urea (43) ^{1}H NMR (500 MHz, DMSO-d^6) δ 9.17 (d, J = 1.9 Hz, 1H), 8.81 (d, J = 1.9 Hz, 1H), 8.78 (s, 1H), 8.75 - 8.74 (m, 3H), 7.86 - 7.85 (m, 1H), 6.79 (d, J = 1.9 Hz, 1H), 6.71 - 6.64 (m, 2H), 3.49 (s, 3H), 3.21 - 3.11 (m, 2H), 2.30 (s, 3H), 1.09 (t, J = 7.2 Hz, 3H). MS (EI$^+$, *m/z*): 404.2 $[M+H]^+$.

1-(1-(5-Chloropyrimidin-2-yl)-6-(1-methyl-2-oxo-1,2-dihydropyridin-4-yl)-1*H*-pyrrolo[3,2-b]pyridin-3-yl)-3-ethylurea (44) ^{1}HNMR (500 MHz, DMSO-d^6): δ 9.10 (s, 1H), 9.05 (s, 2H), 8.83 (s, 2H), 8.60 (s, 1H), 7.80 - 7.86 (m, 1H), 6.85 (s, 1H), 6.70 - 6.69 (m, 2H), 3.43 (s, 3H), 3.12 - 3.16 (m, 2H), 1.07 (t, J = 7.1 Hz, 3H). MS (EI$^+$, *m/z*): 424.0 $[M+H]^+$.

1-Ethyl-3-(1-(5-ethylpyrimidin-2-yl)-6-(1-methyl-2-oxo-1,2-dihydropyridin-4-yl)-1*H*-pyrrolo[3,2-b]pyridin-3-yl)urea (45) ^{1}HNMR (500 MHz, DMSO-d^6): δ 9.15 (d, J = 1.9 Hz, 1H), 8.80 (d, J = 1.9 Hz, 1H), 8.76 (s, 1H), 8.75 - 8.74 (m, 3H), 7.80 - 7.85 (m, 1H), 6.74 (d, J = 1.9 Hz, 1H), 6.69 - 6.61 (m, 2H), 3.49 (s, 3H), 3.25 - 3.11 (m, 2H), 2.27 (q, J = 7.0 Hz, 2H), 1.15 (t, J = 7.0 Hz, 3 H), 1.09 (t, J = 7.2 Hz, 3H). MS (EI$^+$, *m/z*): 418.1 $[M+H]^+$.

1-(1-(5-Bromopyrimidin-2-yl)-6-(1-methyl-2-oxo-1,2-dihydropyridin-4-yl)-1*H*-pyrrolo[3,2-b]pyridin-3-yl)-3-ethylurea (46) ^{1}H NMR (500 MHz, DMSO-d^6) δ 9.11 (s, 1H), 9.05 (s, 2H), 8.85 (s, 2H), 8.69 (s, 1H), 7.87 - 7.86 (m, 1H), 6.80 (s, 1H), 6.70 - 6.69 (m, 2H), 3.49 (s, 3H), 3.18 - 3.16 (m, 2H), 1.09 (t, J = 7.1 Hz, 3H). MS (EI$^+$, *m/z*): 468.0 $[M+H]^+$.

1-(1-(5-Bromopyrimidin-2-yl)-6-(1-(2-hydroxyethyl)-2-oxo-1,2-dihydropyridin-4-yl)-1*H*-pyrrolo[3,2-b]pyridin-3-yl)-3-ethylurea (47) ^{1}H NMR (300 MHz, DMSO-d^6) δ 9.11 (d, J = 2.0 Hz, 1H), 9.04 (s, 2H), 8.83 (d, J = 1.8 Hz, 2H), 8.69 (s, 1H), 7.76 (d, J = 7.0 Hz, 1H), 6.78 (d, J =

1.8 Hz, 1H), 6.66 (dd, J = 7.1, 2.1 Hz, 2H), 4.93 (t, J = 5.4 Hz, 1H), 4.01 (t, J = 5.4 Hz, 2H), 3.67 (d, J = 5.4 Hz, 2H), 3.22 – 3.11 (m, 2H), 1.09 (t, J = 7.2 Hz, 3H). MS (EI$^+$, *m/z*): 498.3 $[M+H]^+$.

Bacterial GyrB and TopoIV IC_{50} Determination. Proteins were obtained from Inspiralis Ltd. (Norwich, United Kingdom). *Sa* gyrase was used at final concentration of 7.5 nM in a solution of 40 mM HEPES-KOH pH 7.6, 10 mM magnesium acetate, 10 mM dithreitol, 50 g/L BSA, 500 mM potassium glutamate, 1% DMSO, 100 mM ATP, and 10 nM linear pBR322 DNA. *Sa* topo IV was used at final concentration of 8.5 nM in a solution of 100 mM Tris pH 7.5, 2 mM magnesium chloride, 1 mM dithreitol, 50 g/L BSA, 200 mM potassium glutamate, 1% DMSO, 300 mM ATP, and 10 nM linear pBR322 DNA. Reactions were carried out in a volume of 10 microliters per well. Reactions were initiated with the addition of ATP and incubated at 20°C for 30 minutes. To quantify ADP concentration, reactions were stopped by addition of 10 microliters of Transcreener ADP2 FP assay reagent and fluorescence polarization measurements were made according to the manufacturer's protocol (Bellbrook Labs, Madison, WI).

MIC Determination. Antibacterial activity of all the compounds was demonstrated by the minimum inhibitory concentrations (MIC) of the compounds against various bacteria measured by the broth microdilution assay performed according to Clinical and Laboratory Standards Institute (CLSI) guidelines with modifications described below. [3] Individual colonies were isolated by streaking frozen glycerol stock of the bacterial species being tested onto rich, non-selective, tryptic soy agar containing 5% sheep's blood (TSAB), and incubated at 37°C for 18-24 hrs. *Streptococcus pneumoniae* strain was streaked on TSAB plates and incubated at 37°C with 5% CO_2 for 18-24 hrs. On the day of the assay, primary cultures were started by inoculating 5-10 colonies from the TSAB plates into ~5 mL of Mueller Hinton Broth (MHB) in 14 mL culture

tubes and incubated at 37°C with aeration (200 rpm) for ~2 hrs until the OD600 was ≥0.1. Inoculum cultures were prepared by standardizing the primary cultures in MHB so that the final inoculum density was ~10^5 colony forming units per milliliter. 50 μL of the diluted inoculum cultures was added to 96 well broth microdilution assay plates along with 50 μL of MHB containing compound (concentrations ranging from 32 – 0.03 μg/mL in two-fold dilutions) for a final volume 100 μL per well with a final culture OD600 of approximately 0.001. For *S. pneumoniae*, 5-10 colonies from TSAB plates were resuspended into MHB to an OD600 of ≥0.1. This material was used to prepare inoculum culture as mentioned above. The final DMSO concentration in the assay plates was 2%. Plates were incubated for 18-20 hours at 37°C with aeration (200 rpm). Assay plates containing *S. pneumoniae* were incubated at 37°C with 5% CO_2 for 18-24 hrs. Following incubation, growth was defined as turbidity that could be detected with the naked eye or achieving minimum OD600 of 0.1. MIC values were defined as the lowest concentration producing no visible turbidity.

X-ray Crystal Structure Determination. Loop-deleted 24 kDa construct of *S. aureus* GyrB was used for X-ray crystallography. Protein crystals were grown using the hanging drop method at pH 7.6, followed by soaking of fragments into the crystallization buffer. Soaking times varied from 16 hours to 33 days. Data were collected using either a Rigaku RA-Micro7 HF rotating anode or at the Diamond Light Source. Structures were solved by molecular replacement using PDB entry 1KZN as a search model. Refinement and model building were completed using REFMAC5 and Coot, respectively.

Table of Contents Graphic

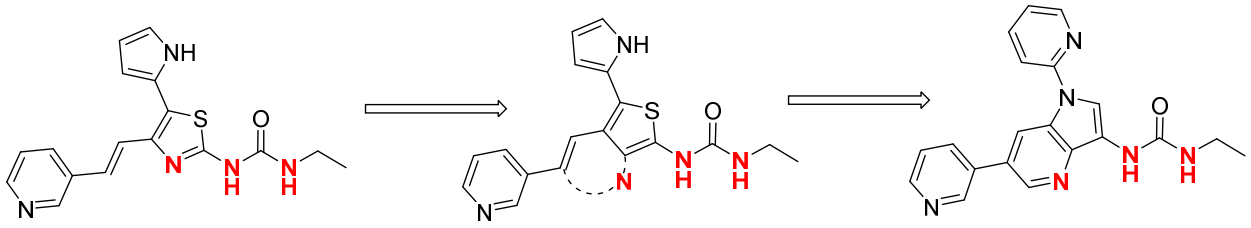

Sa GyrB IC_{50} = 5.8 uM
LE = 0.31 LipE = 2.4

Ring N to displace non-conserved water molecule and serve as HB acceptor

Sa GyrB IC_{50} = 0.14 uM
LE = 0.36 LipE = 4.4

Table of Contents Graphic

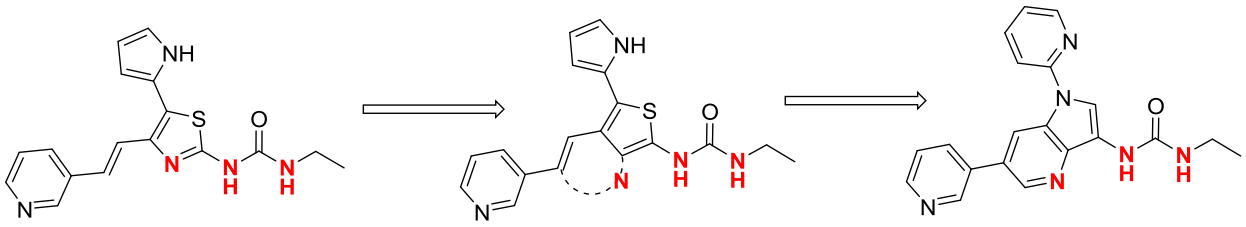

Sa GyrB IC_{50} = 5.8 uM
LE = 0.31 LipE = 2.4

Ring N to displace non-conserved water molecule and serve as HB acceptor

Sa GyrB IC_{50} = 0.14 uM
LE = 0.36 LipE = 4.4